

Multiconverted reflections in marine environments

Taiwen Chen and Don C. Lawton

ABSTRACT

Physical and numerical seismic modeling for multiconverted reflections was undertaken in order to better understand the characteristics of multiconverted reflections for field data from the Canadian Beaufort Sea. Results from seismic modeling suggest that wide-angle, multiconverted events hold promise for imaging reflectors beneath shallow high-velocity layers in marine environments. The multiconverted reflection amplitudes rely strongly on the S-wave velocity in the high-velocity layer, and on the P-wave velocity of the imaged layer. However, the P-wave velocity, the thickness, and the depth of the high-velocity layer do not contribute significantly to multiconverted reflection amplitudes. In the Canadian Beaufort Sea, better imaging for layers underlying the ice-bearing permafrost (high-velocity near surface layer) can be obtained when the multiconverted reflections are considered.

INTRODUCTION

In some sedimentary basins around the world, high-velocity layers (e.g., carbonate, salt, volcanics, anhydrite and permafrost) occurs at or near the surface. Seismic data quality is usually degraded by the high-velocity near-surface layer (HVSL) due to many factors. These factors include energy scattering and seismic wave reverberation in the HVSL, or seismic wave reverberation in the low-velocity layer overlaying the HVSL. Other factors include the source-generated noise, weak energy transmission from the low-velocity layer to the HVSL, etc.

Improved techniques for seismic data acquisition and processing are required to meet the interpretation purposes in areas with an HVSL. Fuller et al. (1988) found that deep reflections could be observed in CDP data by the application of a velocity filter that rejects linear reverberation events from common-source gathers. However, processing can not solve the fundamental problem of the field data quality by itself. Meaningful data must be obtained if a meaningful result is to be obtained (Sheriff, 1991).

Since 1983, much attention has been paid to seismic data acquisition over areas with a high-velocity surface or near-surface layer. The suggested solutions to the problem can be summarized as: seismic array approach (Embree and Roche, 1983; Meister et al., 1989; Pritchett, 1991), receiver patches (Pritchett, 1991), wide-aperture seismic (Jarchow et al., 1991), stack array (Anstey, 1986; Pritchett, 1991), converted-wave approach and shear-wave approach. Purnell et al. (1990) and Pritchett (1991) suggested that better energy transmission between the S mode in the high-velocity layer and the P mode elsewhere could be observed. Fix et al. (1983) showed some successful examples of using shear-waves to get interpretable reflection data.

In Canadian Beaufort Sea, during the Pleistocene glacial cycles, sea levels were 100 m below present (Poley and Lawton, 1991; Poley et al., 1989). Delta plain

deposits were exposed to Arctic climatic conditions. As a result, ice-bearing sediments have accumulated on the Canadian Beaufort Sea shelf with a depth varying from 10 m to 600 m (Poley and Lawton, 1991; Poley et al., 1989). Seismic data recorded in this area affected by ice-bearing permafrost are generally of poor quality (Poley, 1987). Several reasons are causing the poor quality. As Poley (1987) discussed in her thesis, poor penetration (between the high-velocity ice-bearing permafrost and the low velocity surrounding sediments) and reverberation (between the top and the bottom of the ice-bearing permafrost layers) are two of several factors.

Based on ideas from Purnell et al. (1990) and Pritchett (1991), physical and numerical modeling for multiconverted reflections was undertaken for a marine environments with sub-seabottom permafrost. The objective of this study is to show that in marine environments like the Canadian Beaufort Sea, good energy transmission can be observed between S-wave in the ice-bearing permafrost and P-wave elsewhere.

PHYSICAL SEISMIC MODELING

The environment studied here is the marine case, with a high-velocity layer (ice-bearing permafrost) near the water surface. Figure 1 is the schematic diagram showing the geometry for the physical models. In Figure 1, rays 1, 2 and 3 are non-converted reflections, i.e., there is no mode conversion occurring for these rays. However, ray 4 is a typical multiconverted reflection. At larger offsets (normally after passing the critical distance for the incident P-wave), efficient conversion and transmission of S-wave energy through the thin ice-bearing permafrost layer occurs. This energy reconverts to P-wave at the base of the thin layer. Double conversion also occurs for the P-wave energy reflected off the underlying substrate, resulting in the PSPPSP (multiconverted reflection) arrival.

Physical model construction

Five models were constructed to test the ideas discussed above. These models were simplified from previous work by Poley et al. (1989). All these models have four layers: Water, Near surface layer, Water, Basal layer (Figures 2 and 3). The so-called basal layer is the layer to be imaged. In all cases, a thin layer (31 m thick, scaled) was suspended in water above a deeper substrate. This layer simulates a frozen layer with water-saturated unconsolidated sediments. Materials used for the thin layer in each experiment were Plexiglas, PVC Foam and Trabond (Trabond was mixed with glass beads at a ratio of 1:1 by volume). Both the S-wave velocities of Plexiglas and PVC Foam are lower than the P-wave velocity in water, while S-wave velocity in Trabond is greater than the P-wave velocity in water. Both Plexiglas and Trabond were used as high-velocity near surface layers. Materials used for the basal layer were Aluminum, Polystyrene, and Orthodic Foam, which can show the effect of P-wave velocity of the basal layer on the amplitude of multiconverted reflections. However, the extreme case is Orthodic Foam used as the basal layer. Orthodic Foam has a very low P-wave velocity (lower than the P-wave velocity in water). For marine environments, it is not common that the imaged layer has a lower P-wave velocity than that in water. However, by studying this particular model, one may compare the result with other models which has a higher P-wave velocity than that in water. Also, the results from this kind of model may be used for non-marine cases. Results for five models were shown here, which are Plexiglas over Aluminum (Plexiglas was the suspended thin layer, and Aluminum was used as the basal layer, Figure 4), PVC Foam over

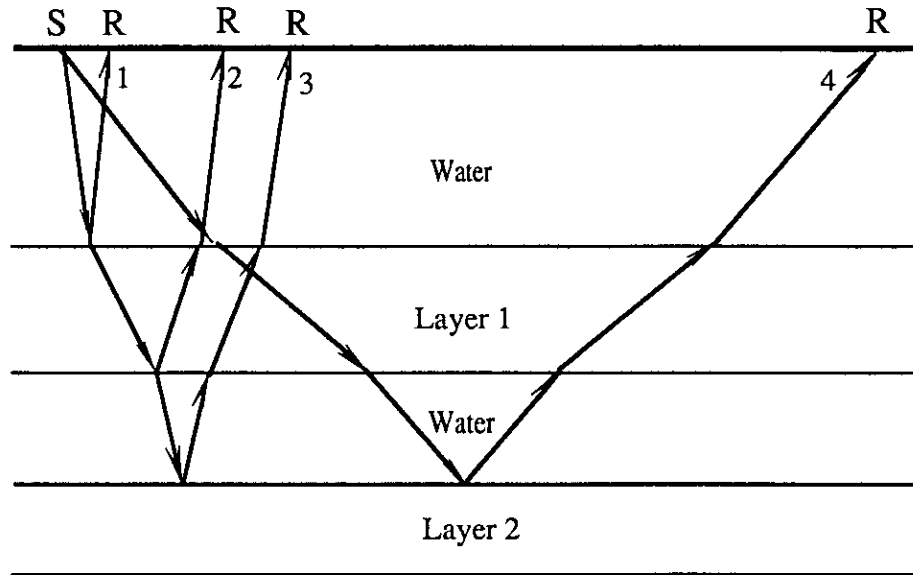


FIG. 1. Schematic diagram showing nonconverted and multiconverted reflections in marine environments. Layer 1 can be a high-velocity layer, such as the ice-bearing permafrost in Canadian Beaufort Sea. S: source; R: receiver; 1: PP; 2: PPPP; 3: P PPPP; 4: PSPPSP (P: P-wave mode; S: S-wave mode).

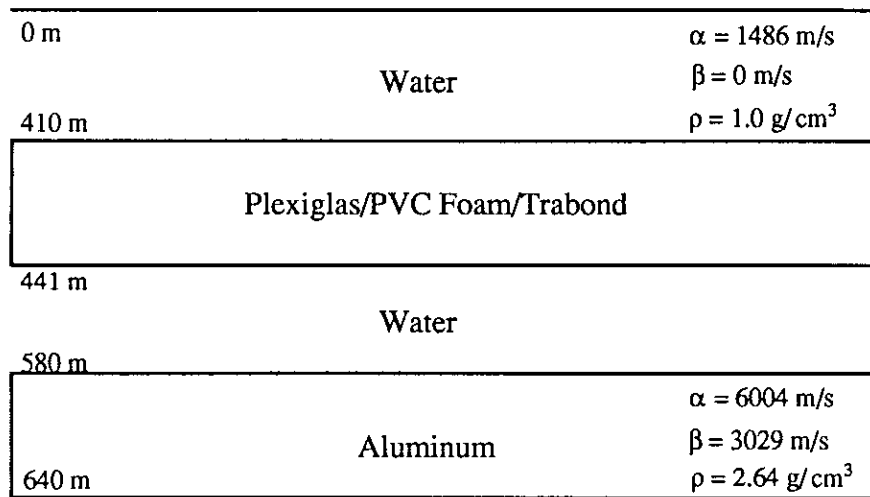


FIG. 2. Schematic diagram showing Models 1-3. Plexiglas was used as the high-velocity near surface layer. α : P-wave velocity; β : S-wave velocity; ρ : density.

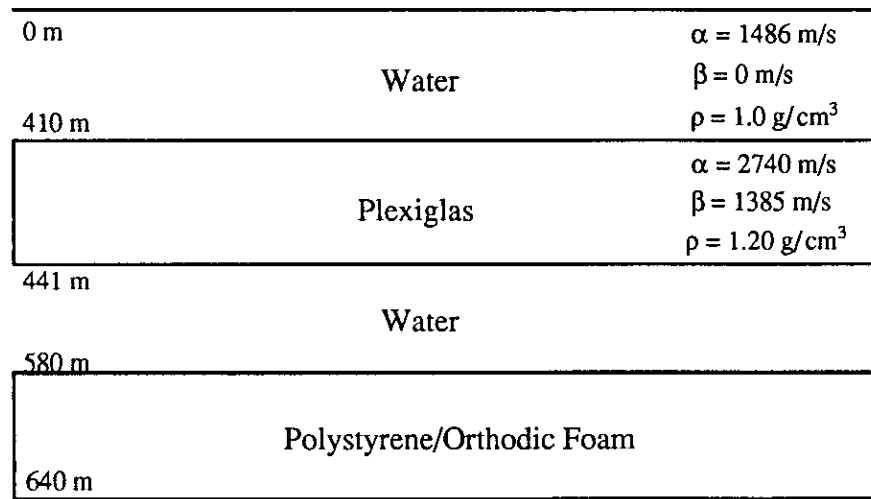


FIG. 3. Schematic diagram showing Models 4-5. PVC Foam was used as the low-velocity near surface layer. α : P-wave velocity; β : S-wave velocity; ρ : density.

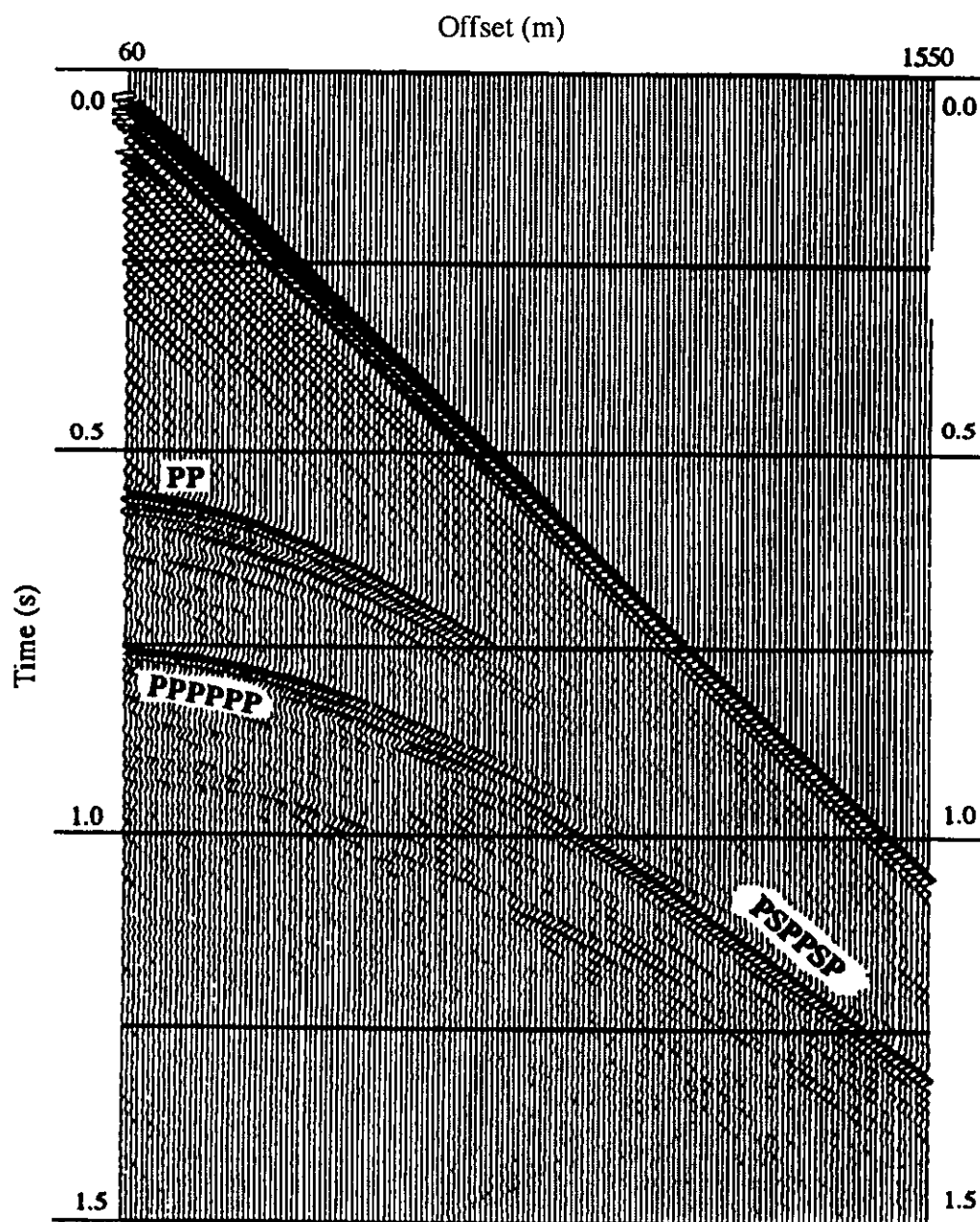


FIG. 4. A shot gather for Model 1. PP: P-wave reflection from the top of Plexiglas; PPPPPP: P-wave reflection from the top of aluminum; PSPPSP: multiconverted reflection from the top of aluminum.

aluminum (Figure 5), Trabond over Aluminum (Figure 6), Plexiglas over Polystyrene (Figure 7), and Plexiglas over Orthodic Foam (Figure 8). Table 1 lists all materials and their physical parameters used in physical modeling.

Table 1: Materials and their physical parameters used in physical modeling.

Compound	Thickness (actual,cm)	Thickness (scaled,m)	Vp (m/s)	Vs (m/s)	σ	ρ (Mg/m ³)
Aluminum	0.62	31	6004	3029	0.33	2.64
Trabond	0.62	31	3010	1733	0.25	1.21
Plexiglas	0.62	31	2740	1385	0.33	1.20
Polystyrene	0.62	31	2063	846	0.40	1.03
Water			1486	0	0.50	1.00
PVC Foam	0.62	31	1100	740	0.10	0.67
Orthodic Foam	0.62	31	1069	591	0.28	0.16

Data acquisition

For acoustic experiments, models were placed in the water-filled seismic tank, and data were collected using small, spherical transducers with a central frequency of 250 kHz. The tank modeling system was developed at the University of Calgary by Cheadle (Cheadle, 1988). The distance and time scale factors for physical modeling are both 1:5000, with a simple velocity scale factor is 1:1. Therefore the central frequency is 50 Hz after scaling. The distances from both transducers to the top of model were about 8.2 cm (410 m scaled).

A 2-D survey was undertaken for these models, and for each record, 150 traces were recorded, with a near offset of 1.2 cm (60 m scaled), a far offset of 31 cm (1550 m scaled), and a group interval of 0.2 cm (10 m scaled). All data were recorded with a sample interval of 100 ns (0.5 ms scaled). Table 2 lists the recording geometry. A total of five lines were collected over the physical models.

Table 2: Scaled geometry for physical modeling

Parameters	Value	Unit
Shots	5	
Traces/shot	150	
Near offset	60	m
Far offset	1550	m
Group interval	10	m
Central frequency	50	Hz.
Samples	4096	
Sample rate	0.5	ms

Results

Figure 4 shows the result for Model 1 which has aluminum as the basal layer, and Plexiglas as the high-velocity near surface layer. In Figure 4, the reflection (PP) from the thin Plexiglas layer diminishes almost to zero amplitude beyond the critical incidence (about 900 m offset). At larger offsets, efficient conversion and transmission

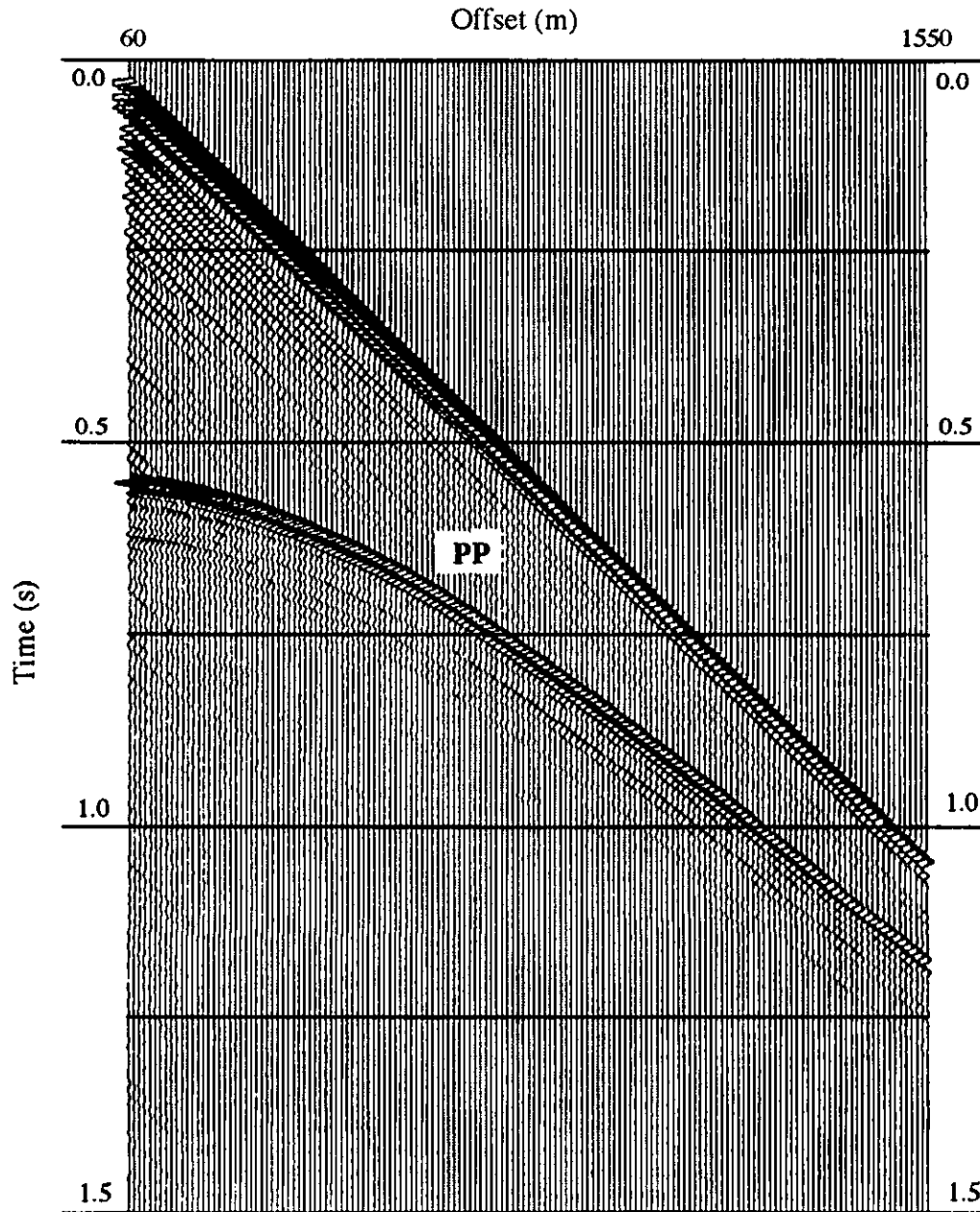


FIG. 5. A shot gather for Model 2. PP: P-wave reflection from the top of PVC Foam.

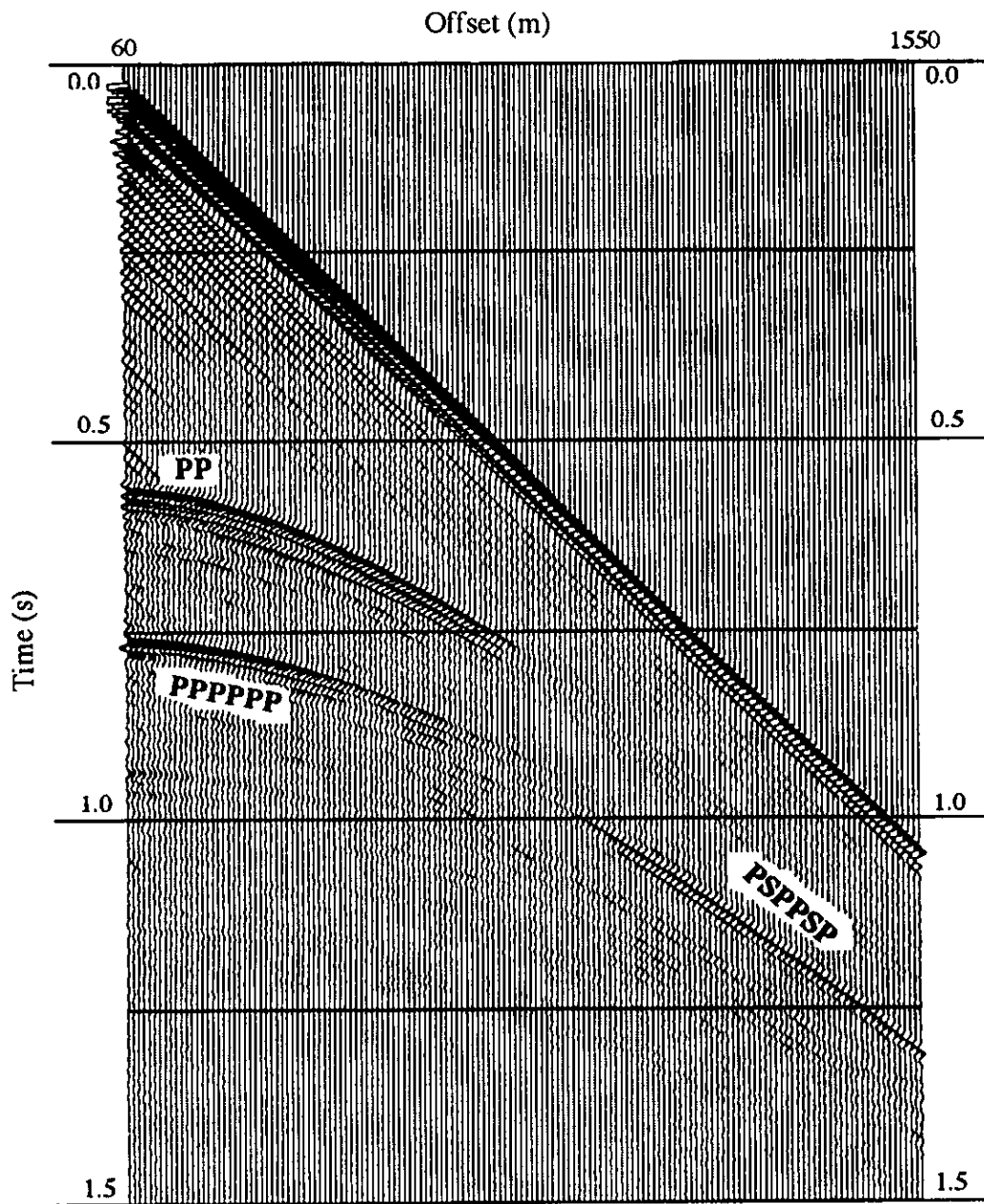


FIG. 6. A shot gather for Model 3. PP: P-wave reflection from the top of Trabond; PPPPPP: P-wave reflection from the top of aluminum; PSPSP: multiconverted reflection from the top of aluminum.

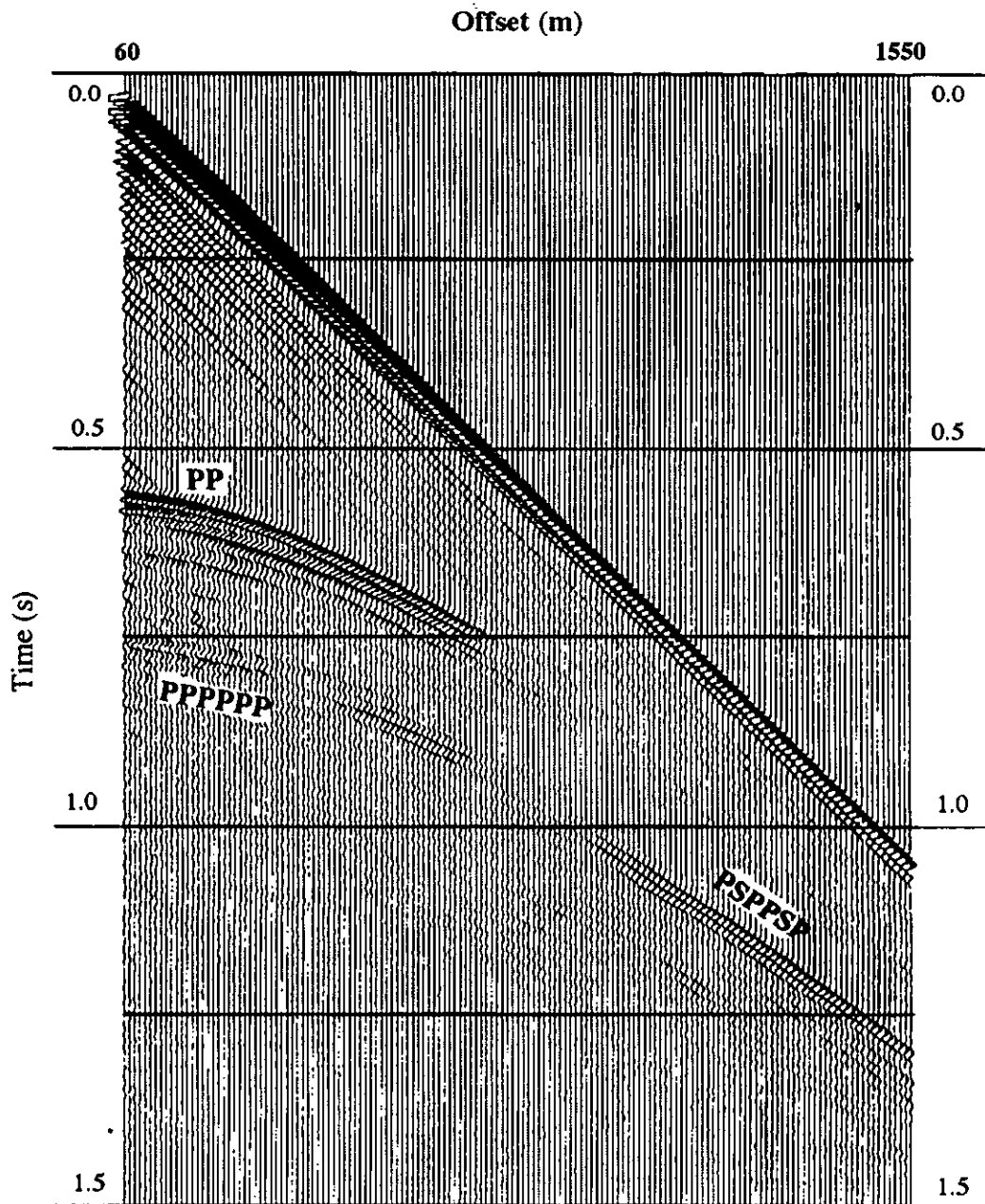


FIG. 7. A shot gather from Model 4. PP: P-wave reflection from the top of Plexiglas; PPPPPP: P-wave reflection from the top of polystyrene; PSPPPSP: multiconverted reflection from the top of polystyrene.

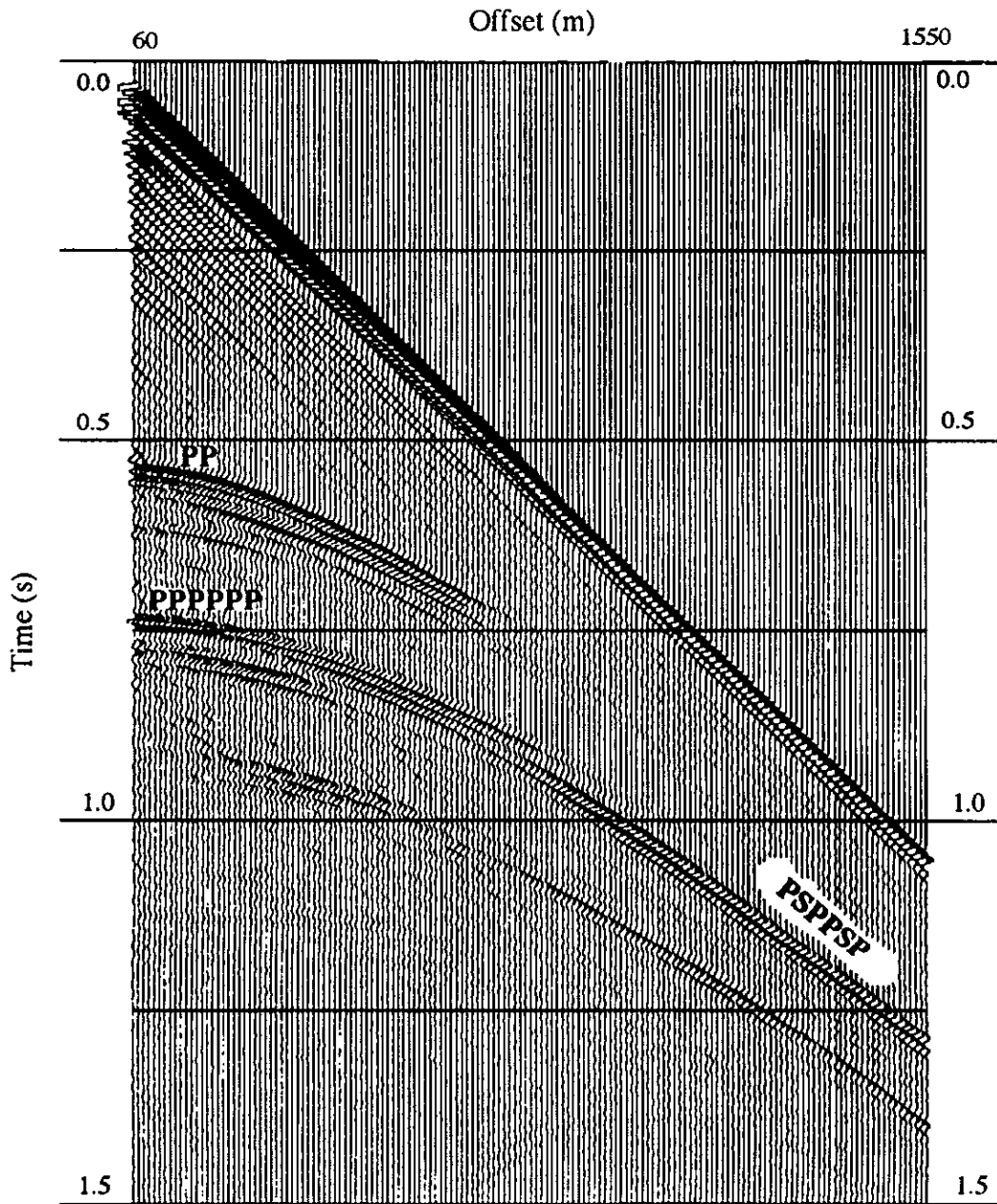


FIG. 8. A shot gather from Model 5. PP: P-wave reflection from the top of Plexiglas; PPPPPP: P-wave reflection from the top of Orthodic Foam; PSPPPSP: multiconverted reflection from the top of Orthodic Foam.

of S-wave energy through the thin Plexiglas layer occurs. This energy reconverts to P-wave at the base of the thin layer. Double conversion also occurs for the P-wave energy reflected off the underlying substrate, resulting in the high-amplitude PSPPSP arrival identified on far offset traces in Figure 4. By contrast, when the low P-wave velocity material PVC Foam was used as the surface layer (Figure 5), the multiconverted wave PSPPSP cannot be identified. This is because the P-wave velocity in PVC Foam is lower than that in water. Therefore, the incident P-wave doesn't reach the critical angle for the reflected P-wave, then there is not much converted Shear mode wave penetrating down through the PVC Foam layer. The converted S-wave energy is neglectable compared with reflected and transmitted P-waves.

In Figure 6, Trabond was used as the near surface layer. The P- and S-wave velocities of this material are higher than those for Plexiglas. The S-wave velocity is much higher than the P-wave velocity in water compared with the case when Plexiglas used as the surface layer. Comparing the multiconverted reflections between Figure 4 and Figure 6, one may conclude that better PSPPSP energy occurs when the S-wave velocity in the HVSL is closer to the P-wave velocity in water.

As mentioned above, model 4 with polystyrene as the basal layer, and Plexiglas as the near-surface layer is the best representative for the permafrost in the Canadian Beaufort Sea. A typical shot gather is shown in Figure 7. In the near offset field, the PPSPPSP event is not clear compared with the far offset field PSPPSP reflection. This would infer that one can obtain a better image by using the far-offset field multiconverted reflection. Comparing the multiconverted reflections between Figure 4 and Figure 7, it seems that better PSPPSP energy occurs when the acoustic impedance difference between water and the basal layer becomes larger. This is expected since the P-wave reflection amplitude off the basal layer will increase as the acoustic impedance contrast increases.

In Figure 8, Orthodic Foam, with a very low P-wave velocity, was used in Model 5. This type of model is not usual in the Canadian Beaufort Sea. But the result could be useful for the non-marine cases. In Figure 8, we can see a very strong PSPPSP reflection energy. This would infer that it is easy to image the layer when its P-wave velocity is lower than that in water.

NUMERICAL SEISMIC MODELING

From the physical modeling, it seems that S-wave velocity of the high-velocity surface layer (HVSL) and the P-wave velocity of the basal layer are key factors for the modeled multiconverted reflection (PSPPSP). It is needed to study detailed effects using synthetic data. For this initial study, only five factors were discussed: S- and P-wave velocities of the HVSL; P-wave velocity of the basal layer; the thickness and the depth of the HVSL. The numerical modeling program was developed at the University of Calgary, and the program was run on Sun Work Stations at the Department of Geology & Geophysics. Transmission and reflection coefficients for the numerical modeling program are calculated using plane wave solutions to Zoeppritz equations, then convolved with Ricker wavelets with a central frequency of 50 Hz.. For all numerical modeling results, transmission losses and geometrical spreading were included, but the attenuation was not.

Model A: Dependence on S-wave velocity in the HVSL

In Model A, the P-wave velocity is kept constant and S-wave velocity is varied for the HVSL. Aluminum was chosen for the basal layer. Table 3 shows physical parameters for the high-velocity layer. S-wave velocities ranging from 714 m/s to 2100 m/s were chosen for studying the effect of the S-wave velocity on the PSPPSP reflection energy. For different S-wave velocities, different synthetic seismograms were obtained. The amplitude of the PSPPSP event was picked and plotted versus incident angle (offset) (Figure 9). In Figure 9, it is clear that the best PSPPSP energy occurs when the S-wave velocity of HVSL is close to the P-wave velocity in water. When the absolute difference between S-wave velocity in HVSL and P-wave velocity in water becomes larger, PSPPSP reflection energy would become smaller.

Table 3: Physical parameters for the HVSL in Model A

Vp (m/s)	Vs(m/s)	σ	ρ (Mg/m ³)
3000	714	0.47	2.0
3000	1477	0.34	2.0
3000	1892	0.17	2.0
3000	2100	0.02	2.0

Model B: Dependence on P-wave velocity in the HVSL

In Model B, the S-wave velocity is kept constant and P-wave velocity is varied for the high-velocity near surface layer. Aluminum was again chosen used as the basal layer. Table 4 shows physical parameters for the HVSL. S-wave velocity was set to be 1480 m/s, which is the same as the P-wave velocity in water. P-wave velocities ranging from 2220 m/s to 4909 m/s were chosen to study the effect of the P-wave velocity on the PSPPSP reflection energy. As for Model A, synthetic gathers were generated for each set of physical parameters and the AVO plot is shown in Figure 10. From Figure 10, it seems that when the S-wave velocity in HVSL is the same as the P-wave velocity in water, changing the P-wave velocity has little effect on the amplitude of the PSPPSP reflection.

Table 4: Physical parameters for the HVSL in Model B

α (m/s)	β (m/s)	σ	ρ (Mg/m ³)
4909	1480	0.45	2.0
2877	1480	0.33	2.0
2563	1480	0.25	2.0
2220	1480	0.10	2.0

Model C: Dependence on the P-wave velocity of the basal layer

In Model C, both the P-wave and S-wave velocities are kept constant for the high-velocity near surface layer, while the P-wave velocity (and the S-wave velocity) in the basal layer are changed. Arbitrary velocities were chosen for the HVSL. The P-wave velocity was set to 3000 m/s, S-wave 1500, with a Poisson's ratio 0.33, and density of 2.0 Mg/m³. Table 5 shows physical parameters for the basal layer. P-wave velocities ranging from 2000 m/s to 6000 m/s were chosen. Figure 11 shows the

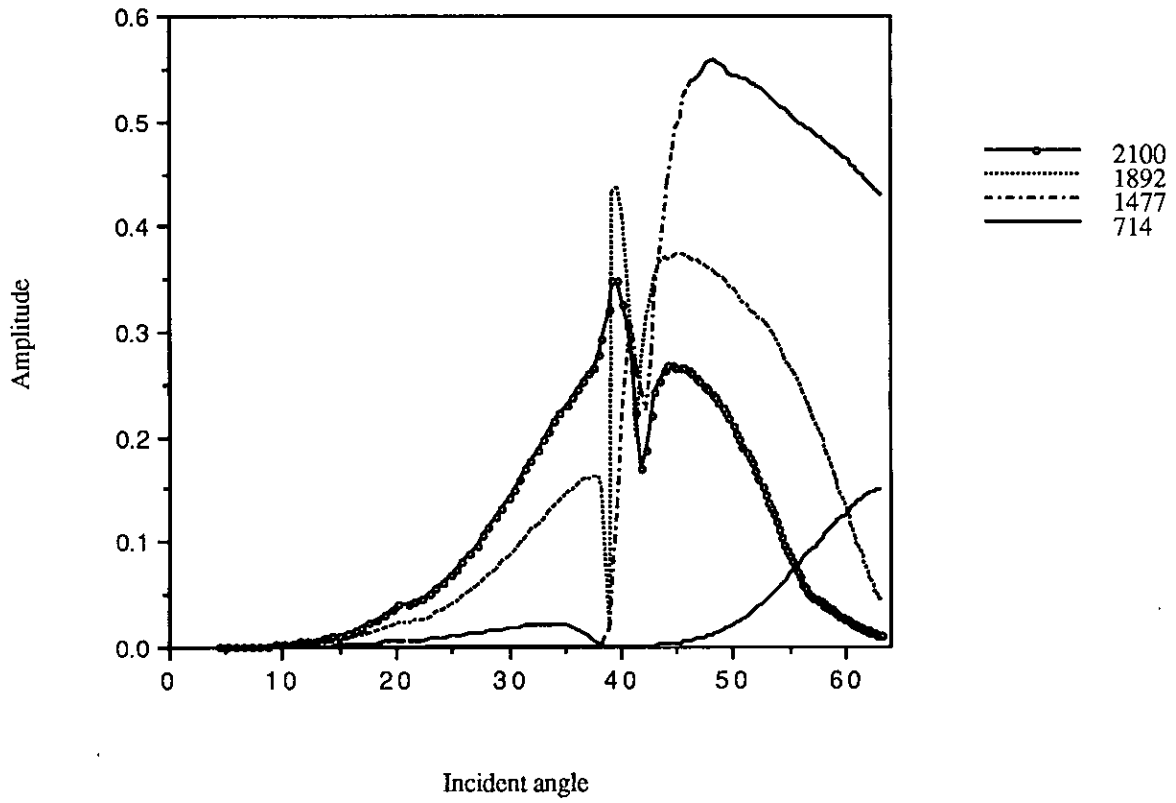


FIG. 9. Effect of S-wave velocity (m/s) of the high-velocity layer.

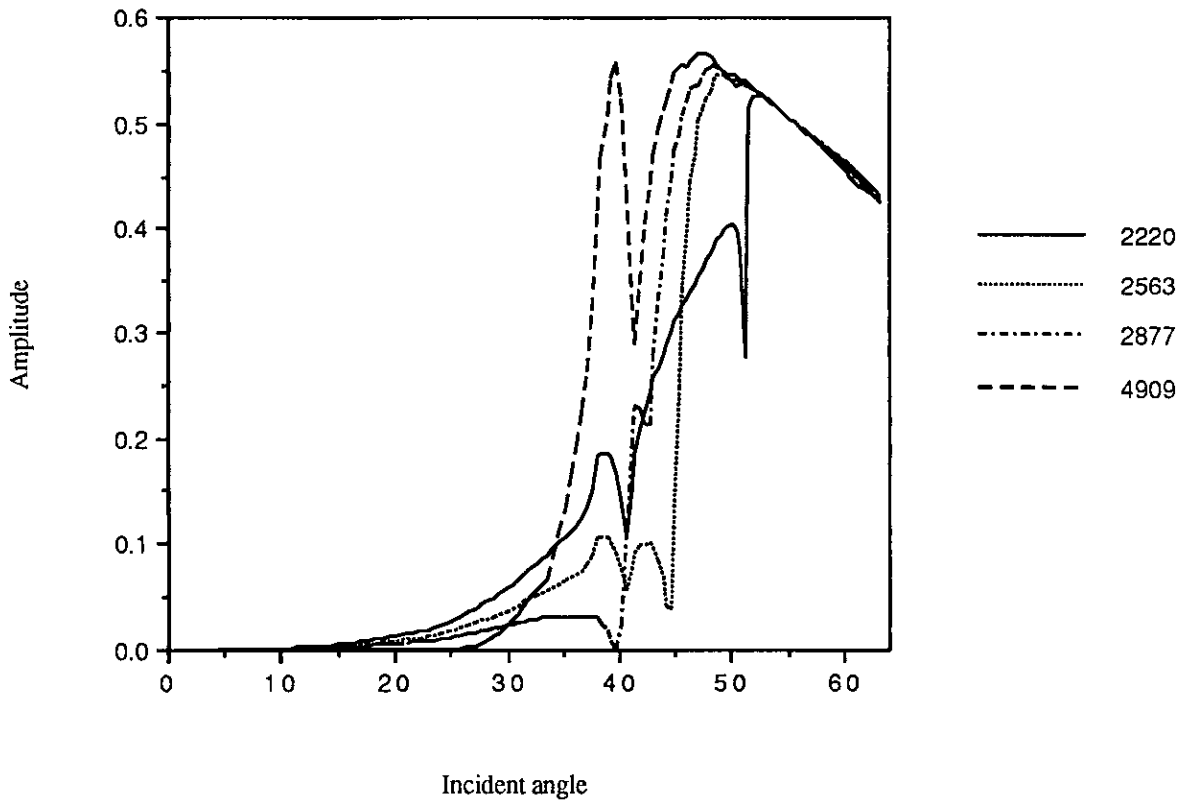


FIG. 10. Effect of P-wave velocity (m/s) of the high-velocity layer.

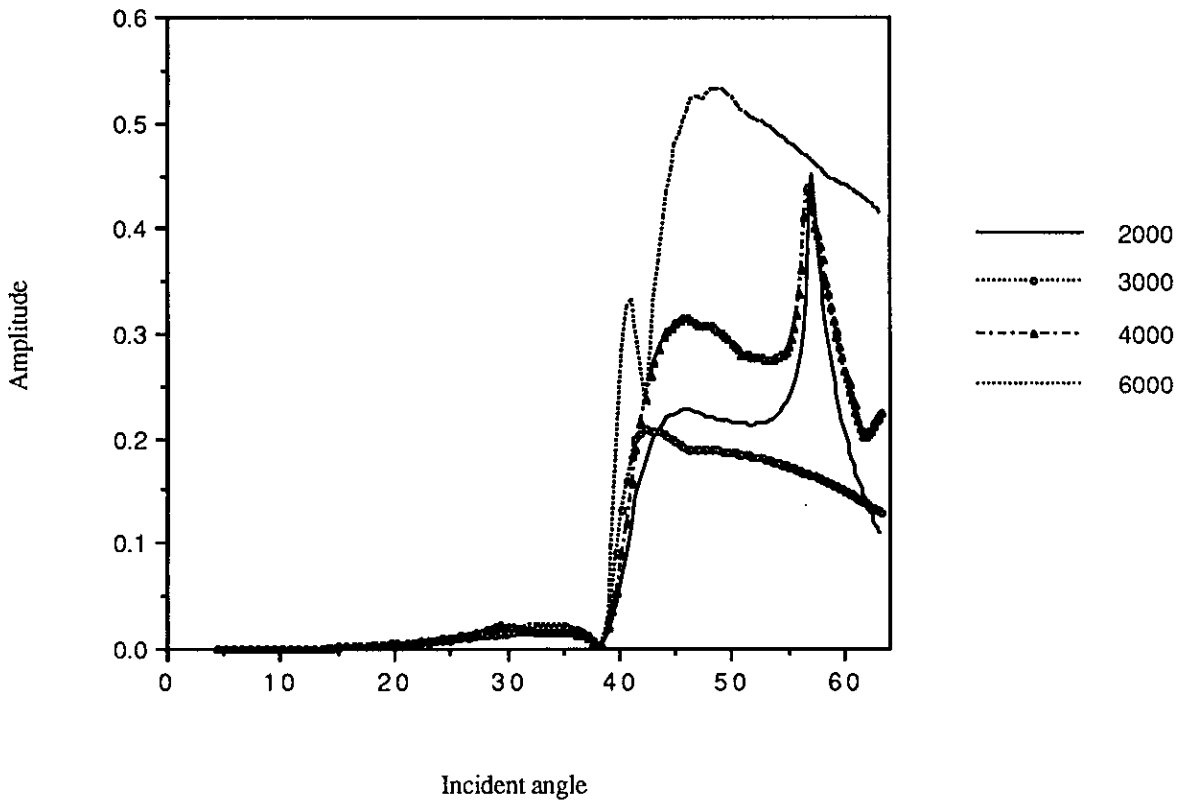


FIG. 11. Effect of P-wave velocity (m/s) in the basal layer.

amplitude versus incident angle diagram for each P-wave velocity of the basal layer. From Figure 11, It seems that increase the P-wave velocity of the basal layer will increase the PSPSP reflection energy, as expected.

Table 5: Physical parameters for the basal layer in Model C

α (m/s)	β (m/s)	σ	ρ (Mg/m ³)
6000	3000	0.33	2.0
4000	2000	0.33	2.0
3000	1500	0.33	2.0
2000	1000	0.33	2.0

Model D: Dependence on thickness of the HVSL

Previous studies (Poley, 1987; Poley and Lawton, 1989; Poley et al., 1991) show that the thickness for the permafrost in the Canadian Beaufort Sea is not constant. The effect of thickness of the HVSL was evaluated with models with thickness of the HVSL of 31 m, 20 m, 10 m, and 5m, respectively. The top of the HVSL was kept constant (410 m for model 4) for each model. Synthetic seismograms were generated and the AVO response plotted in Figure 12. From Figure 12, it is suggested that the thickness does not affect the PSPSP reflection energy. This is mainly due to the fact that the attenuation effect was not involved in the numerical modeling.

Model E: Dependence on depth for the HVSL

Previous studies (Poley, 1987; Poley and Lawton, 1989; Poley et al., 1991) also show that the depth of the top of the permafrost in the Canadian Beaufort Sea varies. Models with different depth for the HVSL were chosen for studying the effect of the depths of the top of the HVSL on the PSPSP reflection energy. The P-wave, S-wave velocities of the ice-bearing permafrost are 3000 and 1700 m/s, respectively. The depths of the high-velocity near-surface layer are 390 m, 250 m, 150 m, and 50 m, respectively. Notice that the thickness of the HVSL was kept constant (31 m) for of these models. As we expected, the AVO plot for the PSPSP event (Figure 13) shows that depth does not affect the PSPSP reflection energy.

FIELD DATA EXAMPLE

The results of the physical and numerical modeling experiments were applied to the analysis of real field data from the Canadian Beaufort Sea. Figure 14 shows a shot gather from a site survey in the Beaufort Sea. The main event of interest in Figure 14 occurs at a reflection time around 0.12 s for the near-offset. It is interpreted as the top of the ice-bearing permafrost. In the middle offset range, there is a strong event occurs around 0.2 s. It is interpreted as the multiconverted reflection (PSSP) from the base of the ice-bearing permafrost. Another event appears at the middle offset with the reflection time around 0.25 s. This is interpreted as the multiconverted reflection (PSPSP) from the top of the layer underlying the ice-bearing permafrost. Figure 15 is the final stack section for the data. The receiver system has 24 groups, with a 12.5 m interval and a near offset of 75 m. The source interval is half of that of the group interval, resulting in a 24 fold section in Figure 15. The data was processed at the University of Calgary, using the ITA (Inverse Theory and Applications) software on the Sun Work Station of the Department of Geology and Geophysics. The standard

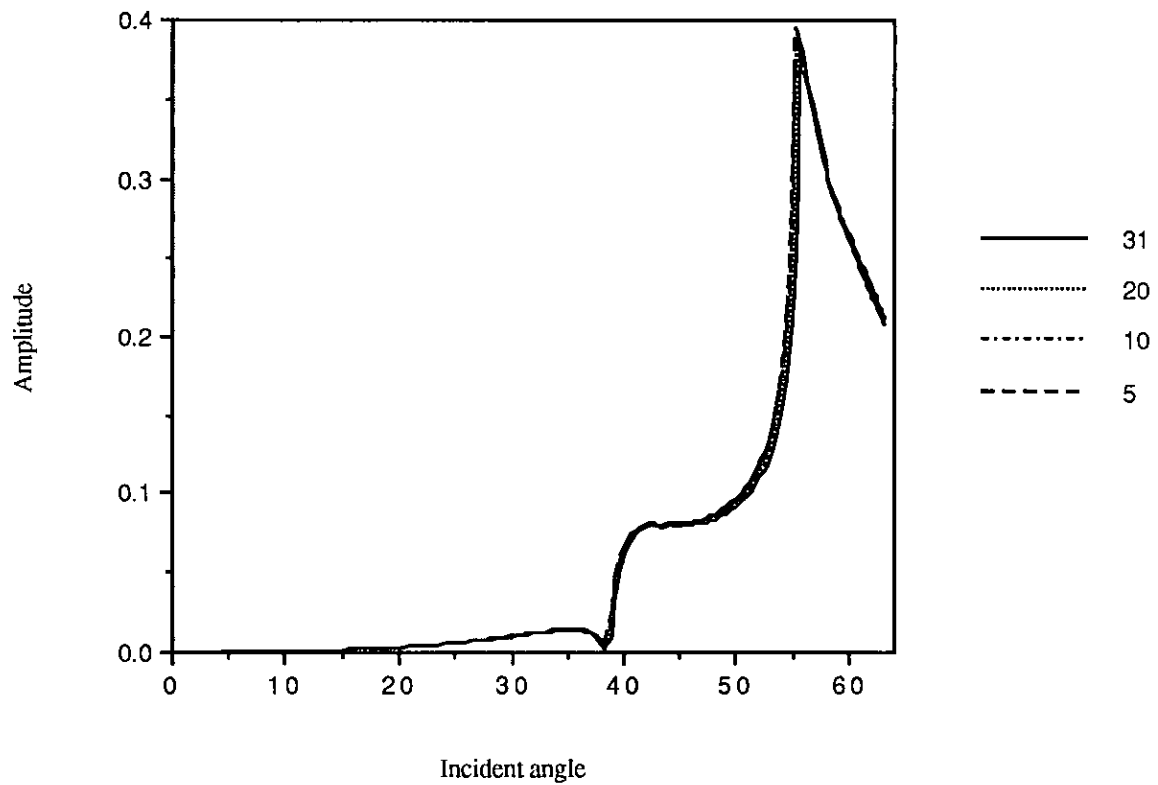


FIG. 12. Effect of the thickness (m) of the high-velocity layer.

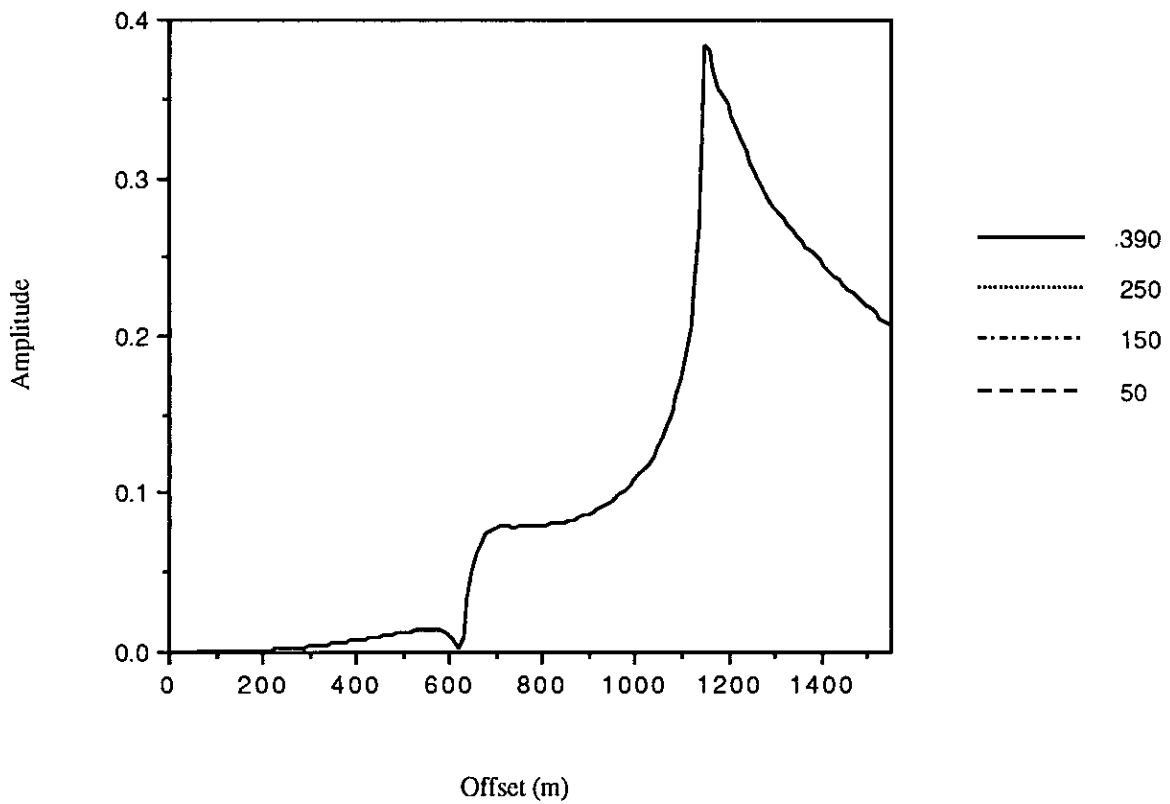


FIG. 13. Effect of the depth (m) of the high-velocity layer. All curves lie upon one another.

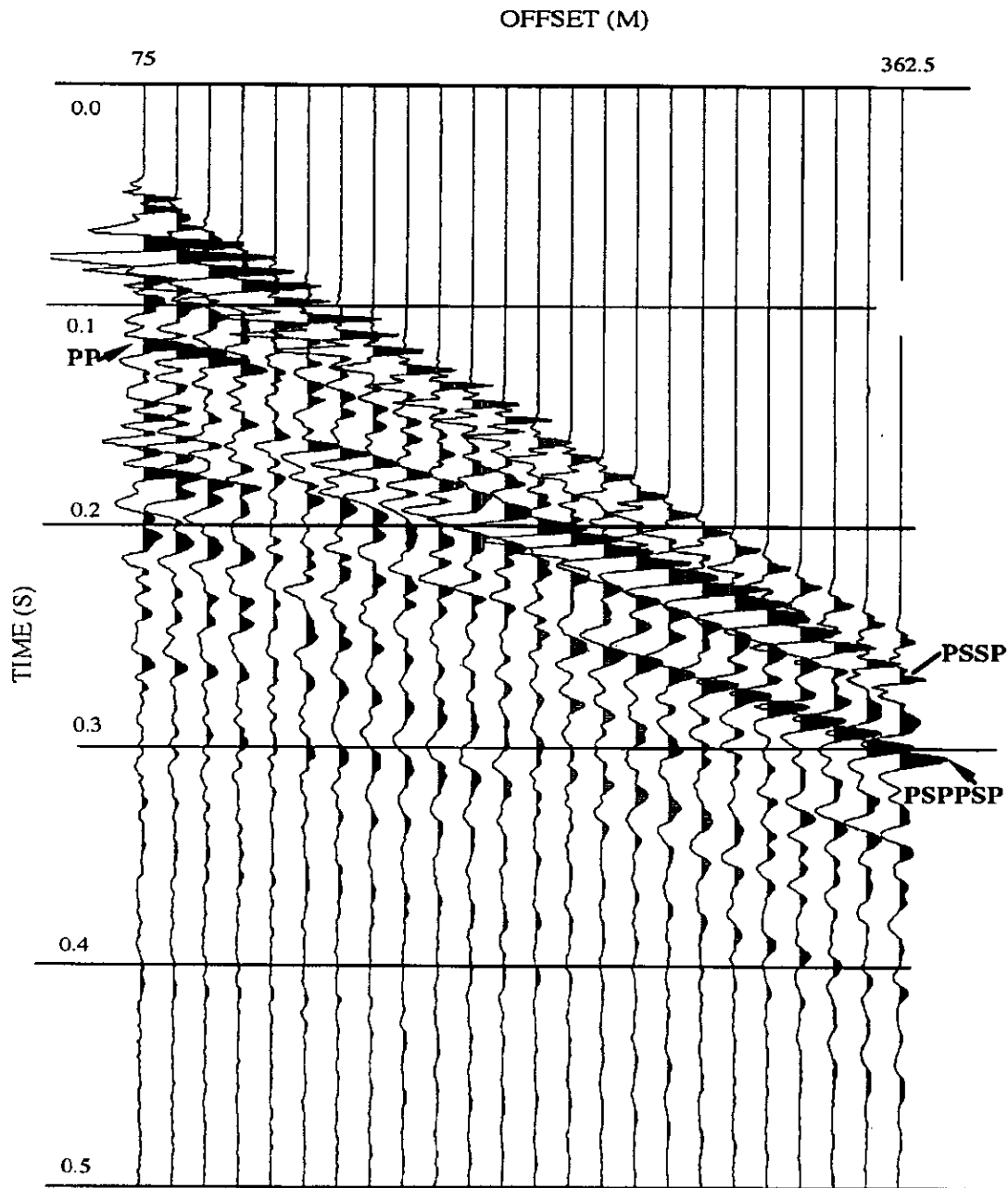


FIG. 14. A shot gather in the Canadian Beaufort Sea. PP: P-wave reflection from the top of the ice-bearing permafrost; PSSP: multiconverted reflection from the base of the ice-bearing permafrost; PSPSP: multiconverted reflection from the top of the layer below the ice-bearing permafrost.

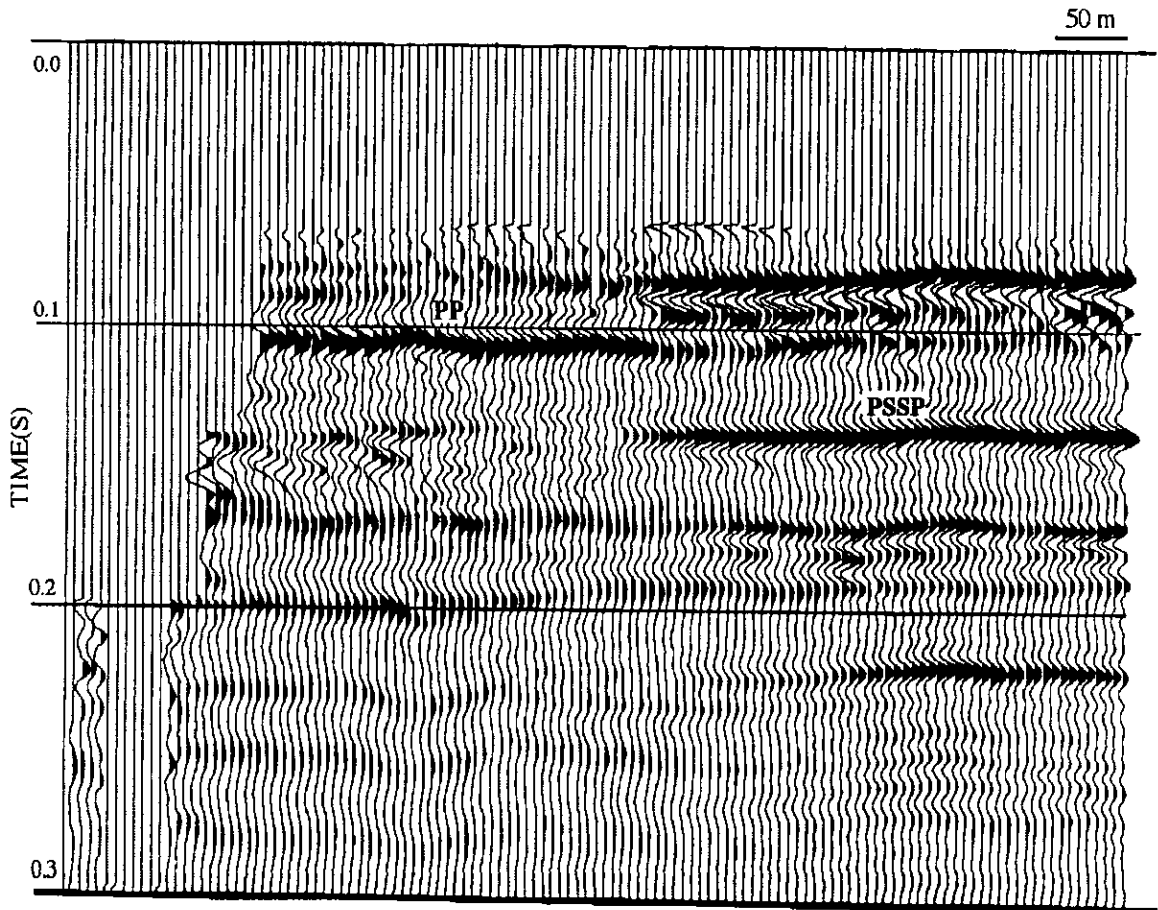


FIG. 15. Final stack section. PP: P-wave reflection from the top of the ice-bearing permafrost; PSSP: multiconverted reflection from the bottom of the ice-bearing permafrost.

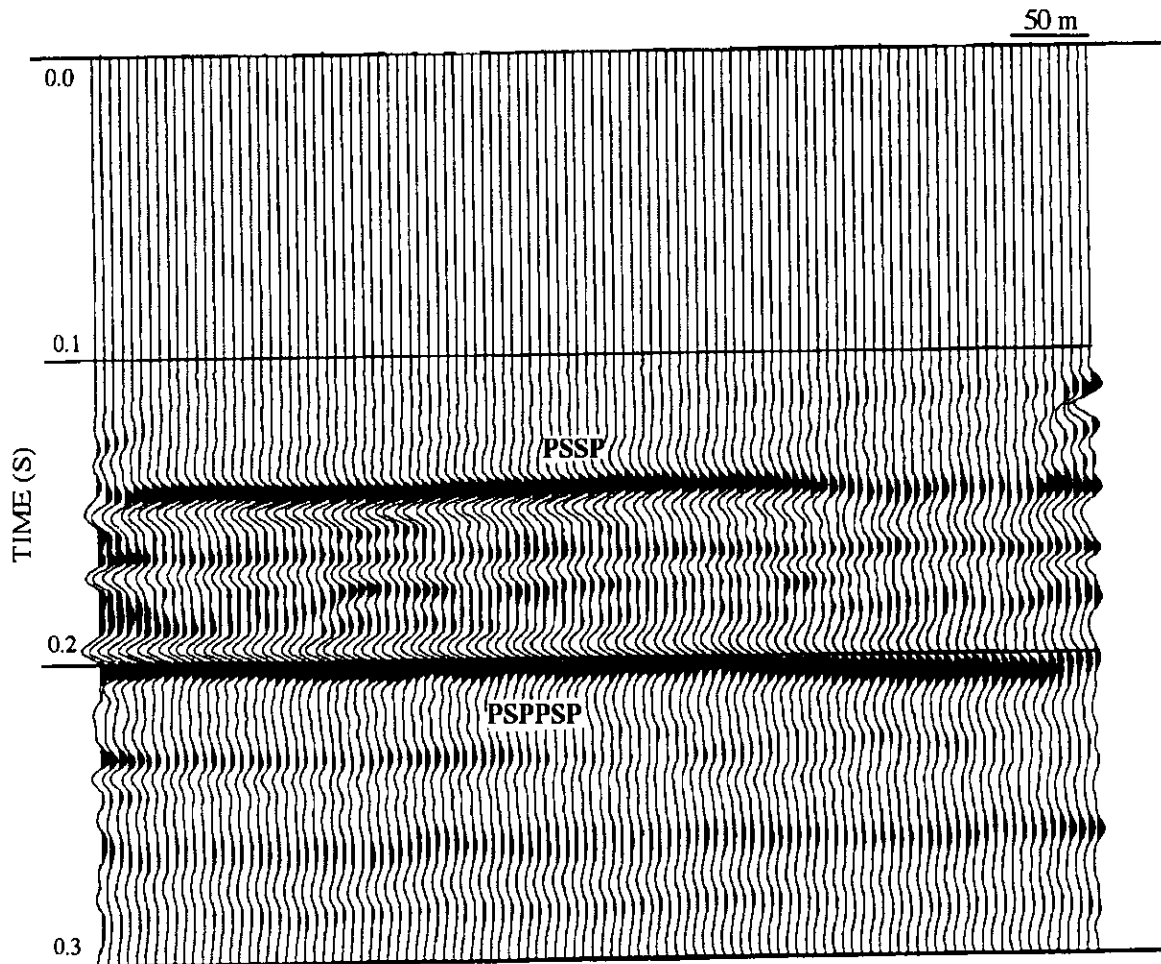


FIG. 16. Stack section with “no-stretch-nmo” applied. PSSP: multiconverted reflection from the base of the ice-bearing permafrost; PSPPSP: multiconverted reflection from the top of the layer below the ice-bearing permafrost.

processing procedure was applied, which includes geometry, CDP sorting, velocity analysis, NMO, and stack.

The event of interest is very shallow (compared with the source to receiver offset), and therefore, stretching occurs after NMO correction. In order to use the useful far-offset information for the multiconverted reflection, "no-stretch-nmo" was also applied for the data. The so called "no-stretch-nmo" actually is one kind of static shift: using the nmo algorithm to calculate the shift amount for each trace for a particular event, then this amount was applied to the data. The output of the shift is kind of NMO correction for a particular event, without stretching the wavelet. Figure 16 shows the final stack section of the same line in Figure 15. Same processing procedure was used, but with "no-stretch-nmo" applied. Besides, only far-offset traces (15 - 24) in Figure 14 were chosen to obtain Figure 16. It is clear that better imaging for the layer underlying the ice-bearing permafrost (high-velocity near surface layer) is obtained when the multiconverted reflections are considered.

CONCLUSIONS

This study has shown that wide-angle, multiconverted reflections hold promise for imaging beneath shallow high-velocity layers in marine environments. These multiconverted reflections rely strongly on the S-wave velocity in the high-velocity layer and the P-wave velocity of the imaged layer. It seems that the P-wave velocity, the thickness, and the depth of the high-velocity layer do not affect the multiconverted reflection amplitude. For the field data from the Canadian Beaufort Sea, better imaging for the layer underlying the ice-bearing permafrost (high-velocity near surface layer) can be obtained when the multiconverted reflections are considered.

ACKNOWLEDGMENTS

We would like to thank Gulf Canada Resources for providing access to the seismic data. Mr. Eric Gallant offered us the technical help in the physical modeling construction and data acquisition. The first author (Chen) also would like to thank CREWES Project and the Department of Geology and Geophysics for the financial assistant as a research and teaching assistant.

REFERENCES

- Anstey, N.A., 1986, Whatever happened to ground roll?: Geophysics: The Leading Edge of Exploration, March, 40-45.
- Anstey, N.A., 1986, Field techniques for high resolution: Geophysics: The Leading Edge of Exploration, April, 26-34.
- Cheadle, S.P., 1988, Applications of physical modeling and localized slant stacking to a seismic study of subsea permafrost: Ph.D. thesis, University of Calgary.
- Embree, P., and Roche, S., 1983, Using vibrators in carbonate areas: presented at the 45th meeting of the European Association of Exploration Geophysicists, Oslo, Norway, June 14-17.
- Fuller, B.N., Pujol, J.M., and Smithson, S.B., 1988, Seismic reflection profiling in the Columbia Plateau: 58th Ann. Internat. Mtg., Soc. Expl. Geophy., Expanded Abstracts, 34-37.

- Jarchow, C.M., Catchings, R.D., and Lutter, W.J., 1991, How Washington crew got good, thrifty seismic in bad data area: *Oil and Gas Journal*, June 17, 54-55.
- Poley, D.F., 1987, Acquisition and processing of high resolution reflection seismic data from permafrost affected areas of the Beaufort Sea Continental Shelf: Ph.D. thesis, University of Calgary.
- Poley, D.F., and Lawton, D.C., 1991, A model study of multichannel reflection seismic data over shallow permafrost in the Beaufort Sea continental shelf: *Jour. Can. Soc. Expl. Geophys.*, 27, 34-42.
- Poley, D.F., Lawton, D.C., and Blasco, S.M., 1989, Amplitude-offset relationships over shallow velocity inversions: *Geophysics*, 54, 1114-1122.
- Pritchett, W.C., 1990, Problems and answers in recording reflections from beneath karst or volcanic surface: 60th Ann. Internat. Mtg., Soc. Expl. Geophy., Expanded Abstracts, 922-925.
- Pritchett, W.C., 1991, Acquiring better seismic data: Chapman and Hall.
- Purnell, G.W., McDonald, J.A., Sekharan, K.K., and Gardner, G.H.F., 1990, Imaging beneath a high-velocity layer using converted waves: 60th Ann. Internat. Mtg., Soc. Expl. Geophy., Expanded Abstracts, 752-755.